

REPORTS

periods [several weeks (11)], during which TTR becomes modified. Comparisons of guanidinium chloride (GdmCl) and guanidinium thiocyanate (GdmSCN) denaturation curves revealed that WT TTR was more resistant to GdmCl denaturation than was T119M, whereas the opposite was true in GdmSCN, as shown previously (9). These differences in midpoints of denaturation can be attributed to differential anion stabilization, suggesting that the true thermodynamic stabilities of these proteins are very similar, although a quantitative analysis is not possible in these chaotropes (22).

A free-energy landscape diagram consistent with all of the experimental data relevant to T119M trans-suppression is shown in Fig. 4C. T119M trans-suppression is principally mediated by destabilization of the dissociative transition state, consistent with positioning of T119M at the dimer-dimer interface. Increasing the dissociative transition-state energy by 3.1 kcal/mol effectively prevents tetramer dissociation because the activation barrier becomes insurmountable (dissociation half-life $t_{1/2}$ increases from ≈ 42 hours to >1500 hours). Small-molecule binding similarly increases the activation barrier associated with tetramer dissociation in a dose-dependent fashion, although this is mediated through tetramer stabilization (Fig. 4A). The extent of stabilization is maximal when the small-molecule dissociation constants K_{d1} and K_{d2} are as low as possible and the concentration of inhibitor is as high as possible. The concentrations used in our experiments for ground-state stabilization are comparable to those observed in plasma for numerous orally available drugs.

Small-molecule binding and trans-suppression increase the activation energy associated with tetramer dissociation, the rate-limiting step of TTR fibril formation. Establishing this analogy is important because it is known that trans-suppression prevents disease in V30M compound heterozygotes (7, 8). Kinetic stabilization of the native state is a particularly attractive strategy, considering the emerging evidence that small misfolded oligomers are neurotoxic (23). Discovering small-molecule binders or developing a trans-suppression approach to tune the energy landscape of other pathologically relevant proteins with a predilection to misfold should now be considered.

References and Notes

1. C. M. Dobson, *Trends Biochem. Sci.* **24**, 329 (1999).
2. A. L. Fink, *Folding Des.* **3**, R9 (1998).
3. D. J. Selkoe, *Science* **275**, 630 (1997).
4. M. S. Goldberg, P. T. Lansbury Jr., *Nature Cell Biol.* **2**, E115 (2000).
5. J. W. Kelly, *Curr. Opin. Struct. Biol.* **6**, 11 (1996).
6. D. R. Jacobson, J. N. Buxbaum, *Adv. Hum. Genet.* **20**, 69 (1991).
7. T. Coelho et al., *J. Rheumatol.* **20**, 179 (1993).
8. T. Coelho et al., *Neuromuscular Disord.* **6**, 27 (1996).

9. P. Hammarström, F. Schneider, J. W. Kelly, *Science* **293**, 2459 (2001).
10. Supporting material is available on Science Online.
11. P. Hammarström, X. Jiang, A. R. Hurshman, E. T. Powers, J. W. Kelly, *Proc. Natl. Acad. Sci. U.S.A.* **99**, 16427 (2002).
12. S. L. McCutchen, Z. Lai, G. Miroy, J. W. Kelly, W. Colon, *Biochemistry* **34**, 13527 (1995).
13. X. Jiang, J. N. Buxbaum, J. W. Kelly, *Proc. Natl. Acad. Sci. U.S.A.* **98**, 14943 (2001).
14. J. C. Sacchettini, J. W. Kelly, *Nature Rev. Drug Discovery* **1**, 267 (2002).
15. G. J. Miroy et al., *Proc. Natl. Acad. Sci. U.S.A.* **93**, 15051 (1996).
16. Small-molecule inhibitors **6** and **8** through **10** do not inhibit TTR amyloidosis when a monomeric variant of TTR (M-TTR) (24) is employed for acid-mediated amyloid fibril formation studies (Fig. 2F), demonstrating that the inhibitors mediate amyloid inhibition through tetramer binding (Fig. 2, E and F). Inhibitor **7** slightly inhibits fibril formation from M-TTR because it drives a small fraction of M-TTR into a tetrameric quaternary structure (Fig. 2F).
17. T. Klabunde et al., *Nature Struct. Biol.* **7**, 312 (2000).
18. The calculated and observed amplitude changes do not match the populations of $T \cdot I_1$ and $T \cdot I_2$ displayed in Fig. 3, C and D, exactly in all cases owing to the fact that K_{d1} , K_{d2} , and the free energy of stabilization resulting from the binding of one (ΔG_1) and two (ΔG_2) ligands were all evaluated under physiological conditions (Fig. 1B), and the experiments described here were carried out in 6 M urea.
19. $\Delta G_1 = RT \ln([T \cdot I]/[T]) = RT \ln([I]/K_{d1})$ and $\Delta G_2 = RT \ln([T \cdot I_2]/[T]) = RT \ln([I]^2/(K_{d1} \cdot K_{d2}))$.
20. J. V. Schloss, *Acc. Chem. Res.* **21**, 348 (1988).
21. D. Baker, J. L. Sohl, D. A. Agard, *Nature* **356**, 263 (1992).
22. P. Hammarström, X. Jiang, S. Deechongkit, J. W. Kelly, *Biochemistry* **40**, 11453 (2001).
23. Emerging data from the laboratories of S. Lindquist (25), D. Selkoe (26), C. Dobson (27), P. Lansbury (28), G. Krafft (29), and others reveal that oligomeric aggregates of proteins with a tendency to misfold and misassemble are more toxic to cells than are the insoluble aggregates with high molecular weight (e.g., amyloid fibrils and the scrapie form of the prion protein, PrP^{Sc}).
24. X. Jiang et al., *Biochemistry* **40**, 11442 (2001).
25. J. Ma, S. Lindquist, *Science* **298**, 1785 (2002); published online 17 October 2002 (10.1126/science.1073619).
26. D. M. Walsh et al., *Nature* **416**, 535 (2002).
27. M. Bucciantini et al., *Nature* **416**, 507 (2002).
28. H. A. Lashuel et al., *Nature* **418**, 291 (2002).
29. W. L. Klein et al., *Trends Neurosci.* **24**, 219 (2001).
30. V. B. Oza et al., *J. Med. Chem.* **45**, 321 (2002).
31. S. A. Peterson et al., *Proc. Natl. Acad. Sci. U.S.A.* **95**, 12956 (1998).
32. H. E. Purkey, J. W. Kelly, unpublished results.
33. H. E. Purkey, M. I. Dorrell, J. W. Kelly, *Proc. Natl. Acad. Sci. U.S.A.* **98**, 5566 (2001).
34. We thank NIH (grant DK 46335), The Skaggs Institute of Chemical Biology, and the Lita Annenberg Hazen Foundation for financial support; R. A. Lerner and I. Wilson for useful suggestions; and the Wenner-Gren Foundation for a postdoctoral fellowship (P.H.).

Supporting Online Material

www.sciencemag.org/cgi/content/full/299/5607/713/DC1

SOM Text

Figs. S1 and S2

References and Notes

21 October 2002; accepted 13 December 2002

ARGONAUTE4 Control of Locus-Specific siRNA Accumulation and DNA and Histone Methylation

Daniel Zilberman,¹ Xiaofeng Cao,¹ Steven E. Jacobsen,^{1,2*}

Proteins of the ARGONAUTE family are important in diverse posttranscriptional RNA-mediated gene-silencing systems as well as in transcriptional gene silencing in *Drosophila* and fission yeast and in programmed DNA elimination in *Tetrahymena*. We cloned ARGONAUTE4 (AGO4) from a screen for mutants that suppress silencing of the *Arabidopsis SUPERMAN (SUP)* gene. The *ago4-1* mutant reactivated silent *SUP* alleles and decreased CpNpG and asymmetric DNA methylation as well as histone H3 lysine-9 methylation. In addition, *ago4-1* blocked histone and DNA methylation and the accumulation of 25-nucleotide small interfering RNAs (siRNAs) that correspond to the retroelement *AtSN1*. These results suggest that AGO4 and long siRNAs direct chromatin modifications, including histone methylation and non-CpG DNA methylation.

Members of the ARGONAUTE (AGO) protein family are important in RNA-mediated silencing systems such as posttranscriptional gene silencing (PTGS) in plants, RNA interference in animals, and quelling in fungi (1, 2). These systems use a ribonuclease III enzyme, DICER, to generate 21- to 22-nucleo-

otide (nt) small interfering RNAs (siRNAs), which target the destruction of homologous RNA. In plants, PTGS is often associated with RNA-directed methylation of the corresponding DNA (3) and, conversely, plant chromatin mutants such as *ddm1* and *met1* can affect PTGS (4). In addition, AGO family members have recently been implicated in histone modifications and transcriptional gene silencing. In fission yeast, deletion of *argonaute*, *dicer*, and RNA-dependent RNA polymerase homologs causes transcriptional derepression and loss of histone H3 lysine-9

¹Department of Molecular, Cell, and Developmental Biology, ²Molecular Biology Institute, University of California, Los Angeles, CA 90095-1606.

*To whom correspondence should be addressed. E-mail: jacobsen@ucla.edu.

(H3K9) methylation (5, 6). In *Tetrahymena*, TIWI, a member of the PIWI subfamily of AGOs, is required for programmed DNA elimination, which is associated with 28-nt siRNAs and histone H3K9 methylation (7, 8). Finally, *Drosophila* PIWI is required for both posttranscriptional and transcriptional repression of alcohol dehydrogenase transgenes (9).

The *clark kent* (*clk*) mutants are epigenetic alleles of the *Arabidopsis* *SUP* gene caused by *SUP* gene silencing and extensive DNA methylation of CpG, CpNpG (where N is either A, C, T, or G), and asymmetric (CpHpH, where H is either A, C, or T) cytosines (10). The *clk* mutants are recessive and meiotically heritable, suggesting a primarily chromatin-based gene-silencing mechanism. Indeed, the initiation of *SUP* silencing requires the DRM2 de novo DNA methyltransferase (11). Furthermore, by screening for suppressors of the *clk-st* allele, we isolated two chromatin modification enzymes required for the maintenance of *SUP* gene silencing, *CHROMOMETHYLASE3* (*CMT3*) and *KRYPTONITE* (*KYP*). *CMT3* encodes a DNA methyltransferase, and *KYP* encodes a histone H3K9-specific protein methyltransferase (12, 13). *kyp* and *cmt3* mutants both cause a loss of CpNpG methylation at *SUP* and all other loci tested. Here we describe the cloning of a third *clk-st* suppressor mutation in the *AGO4* gene.

We identified one recessive allele of a *clk-st* suppressor gene that mapped to chromosome II. Other than suppression of *SUP* silencing, we did not observe morphological defects in the homozygous mutant. By se-

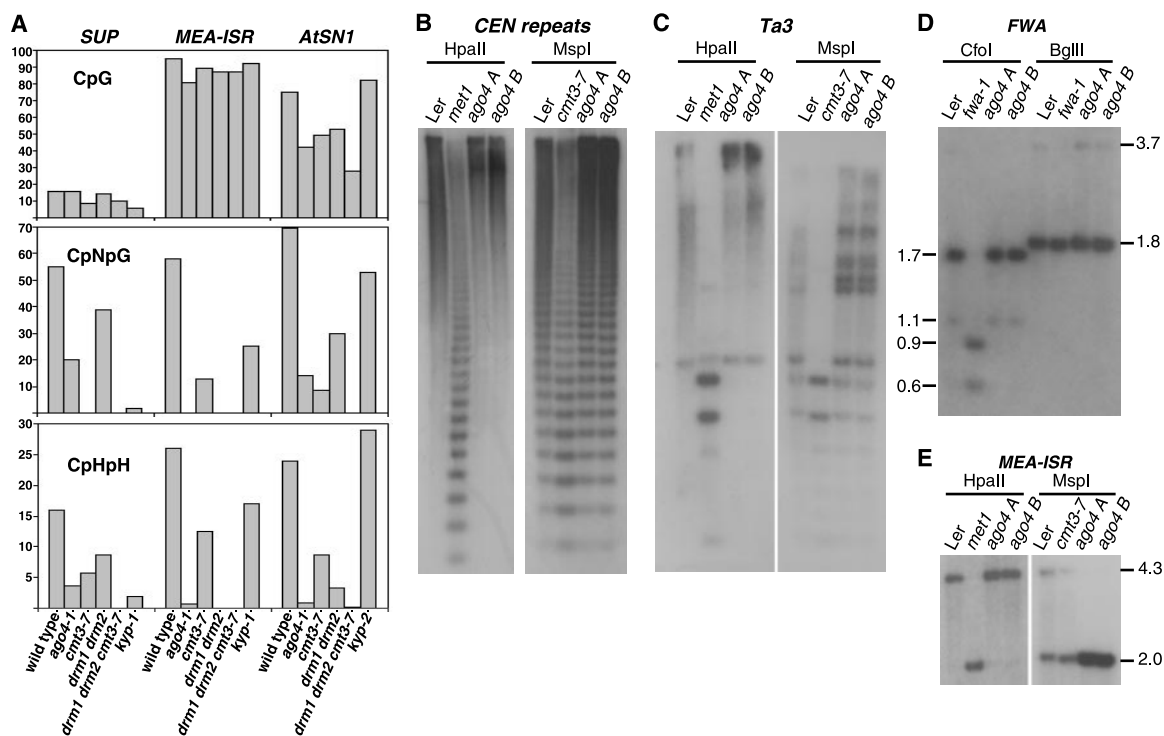
quencing candidate genes, we identified a mutation in the *AGO4* gene, previously named on the basis of its sequence similarity to *AGO1* (1). The mutation destroyed a splice acceptor site, causing a deletion and frameshift that terminated translation after 595 amino acids (fig. S1). The *AGO4*s comprise a conserved family of eukaryotic genes (fig. S1) containing two domains of unknown function: an NH₂-terminal PAZ domain and a COOH-terminal PIWI domain (14). Because the frameshift deleted almost the entire PIWI domain, the mutation is likely to cause severe loss of *AGO4* function. To confirm that the suppressor mutation is within *AGO4*, we transformed mutant plants with the *AGO4* gene and found that the original *clk-st* phenotype was restored. Thus we named this suppressor mutation *ago4-1*.

We analyzed the effect of *ago4-1* on *SUP* DNA methylation using bisulfite genomic sequencing (Fig. 1A and table S1). Whereas CpG methylation levels were unchanged, *ago4-1* showed a 2.8-fold reduction in CpNpG and a 4.5-fold reduction in asymmetric methylation. This methylation phenotype was similar to that of the *cmt3* and *kyp* mutants, except that *cmt3* and *kyp* showed a stronger reduction of CpNpG methylation than did *ago4-1*. We previously found that, at all loci tested, *cmt3* and *kyp* showed a reduction of CpNpG methylation but not of CpG methylation (12, 13). Therefore, we used Southern blot analysis with methylation-sensitive restriction enzymes to assay the effect

of *ago4-1* on both CpG and CpNpG methylation at three additional loci: the 180-base-pair (bp) centromeric repeat (*CEN*) sequence (Fig. 1B), the *Ta3* retrotransposon (Fig. 1C), and the *FWA* gene (Fig. 1D). The *ago4-1* mutation did not affect either CpNpG or CpG methylation levels at these loci. The *FWA* locus also contains a substantial amount of asymmetric methylation (15), and bisulfite sequencing of *FWA* showed that the *ago4-1* mutation did not reduce this methylation. Thus, the methylation phenotype of *ago4-1* is locus-specific and different than that of the *cmt3* and *kyp* mutants.

We found three other loci at which *ago4-1* did have an effect on DNA methylation: *MEA-ISR*, *AtSN1*, and *AtMu1*. *MEA-ISR* is an approximately 183-bp sequence present in seven direct repeats in an intergenic region adjacent to the imprinted *MEDEA* gene (16). In the wild type, *MEA-ISR* locus contains 95% CpG, 58% CpNpG, and 26% asymmetric methylation (Fig. 1A and table S1). *ago4-1* essentially eliminated the CpNpG and asymmetric methylation but did not affect the CpG methylation (Fig. 1A). We used Southern blot analysis with methylation-sensitive restriction enzymes to confirm these results. We found that CpNpG methylation was eliminated in *ago4-1* but that CpG methylation was unaffected (Fig. 1E). *AtSN1* is a retrotransposon sequence previously shown to be methylated (17). We found that the wild-type *AtSN1* locus contains 75% CpG, 70% CpNpG, and 24% asymmetric methylation (Fig. 1A and table S1). *ago4-1* greatly reduced

Fig. 1. Methylation analysis of the *ago4-1* mutant. (A) Bisulfite sequencing results show the percent methylation in different sequence contexts of *SUP*, *MEA-ISR*, and *AtSN1* in different mutant backgrounds. (B to E) Southern blot analysis of genomic DNA cut with the indicated restriction enzyme and probed with (B) *CEN*, (C) *Ta3*, (D) *FWA*, and (E) *MEA-ISR* probes. Probes and restriction maps are described in (16). *Hpa* II and *Msp* I recognize the sequence CCGG. *Hpa* II is inhibited by methylation of either cytosine and allows detection of CpG and CpNpG methylation, whereas *Msp* I is only inhibited by methylation of the outer cytosine, allowing detection of CpNpG methylation only. *Cfo* I detects CpG methylation and *Bgl* II detects CpNpG methylation. *ago4 A* and *B* are different isolates of *ago4-1*. Controls include the *met1* and *cmt3-7* mutants in (B), (C), and (E), and the hypomethylated *fwa-1* mutant (15) in (D).



REPORTS

the non-CpG methylation to 14% CpNpG and 0.8% asymmetric methylation. The *AtMu1* sequence is the 3'-terminal inverted repeat of the *Arabidopsis* DNA transposon *Mu1* (18). We found that wild-type *AtMu1* shows 58% CpG, 35% CpNpG, and 11% asymmetric methylation. The *ago4-1* mutation did not affect the CpG methylation but reduced the CpNpG methylation to 19% and the asymmetric methylation to 4.8% (table S1).

The locus-specific effect of *ago4-1* shows that both *AGO4*-dependent and *AGO4*-independent mechanisms control non-CpG methylation.

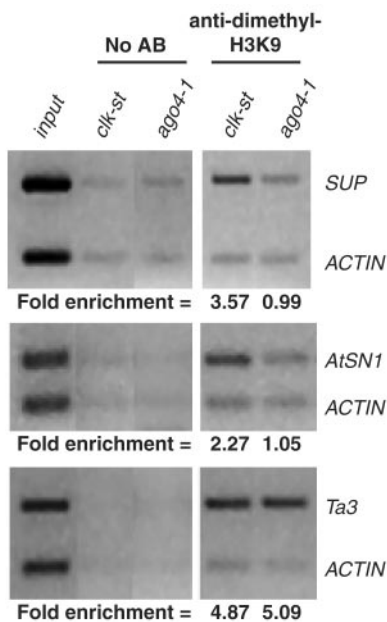


Fig. 2. ChIP analysis of H3K9 methylation, showing multiplex polymerase chain reaction analyses of *SUP*, *AtSN1*, and *Ta3* together with *ACTIN*, a locus with a low level of H3K9 methylation (19). The input is *clk-st* chromatin before immunoprecipitation. "No AB" lanes are control immunoprecipitations with no antibody. The fold enrichment of the *SUP*, *AtSN1*, and *Ta3* signal over the *ACTIN* signal is shown.

CEN, *Ta3*, and *FWA* rely on an *AGO4*-independent mechanism, *MEA-ISR* on an *AGO4*-dependent mechanism, and *SUP*, *AtSN1*, and *AtMu1* on both mechanisms. One explanation for *AGO4*-independent non-CpG methylation is that another *AGO* gene (nine of which are present in the *Arabidopsis* genome) could act redundantly with *AGO4*. Alternatively, pathways that do not involve *AGO* genes could function at some loci. For instance, if *AGO4*'s primary role is to establish methylation, effects will only be visible at loci that require frequent establishment.

A comparison of the methylation phenotype of *ago4-1* with those of mutants of *CMT3* and *DRM*, the two types of DNA methyltransferase genes known to control non-CpG methylation, did not show a simple relationship (Fig. 1A). In particular, *ago4-1* mimicked the *drm1 drm2* double mutant at *MEA-ISR* (16). However, at both *SUP* and *AtSN1*, *ago4-1* showed a reduction in CpNpG methylation that was intermediate between the effects of the *cmt3-7* and *drm1 drm2* mutants and a reduction of asymmetric methylation that was stronger than the effect of either (Fig. 1A). These results suggest that both *CMT3* and *DRM* are involved in *AGO4*-dependent methylation.

To determine the relationship between *AGO4*, *KYP*, and *CMT3*, we performed chromatin immunoprecipitation (ChIP) experiments to examine histone H3K9 methylation levels at *SUP*. We previously found that *kyp*, but not *cmt3*, reduced H3K9 methylation at *SUP* (19), suggesting that *CMT3* acts downstream of *KYP*, because of targeting of *CMT3* to methylated histones (13). Figure 2 shows that *ago4-1* reduced H3K9 methylation of *SUP* relative to the wild-type strain *clk-st*. The simplest interpretation of these results is that *AGO4* acts upstream of *KYP* to target H3K9 methylation. We also found that *ago4-1* reduced H3K9 methylation at *AtSN1*, a locus where *ago4-1* also reduced DNA

methylation (Fig. 2). However, *ago4-1* did not reduce H3K9 methylation of *Ta3* (Fig. 2) or of the *CEN* repeats, where *ago4-1* showed no DNA methylation effect. Thus, the effects of *ago4-1* on H3K9 methylation are locus-specific and correlate with effects on DNA methylation.

We tested whether *AGO4* function is associated with siRNAs by probing Northern blots of RNA preparations that had been enriched for small RNAs. *AtSN1* was recently shown to be associated with a newly discovered class of long (approximately 25-nt) siRNAs (17). We could easily detect *AtSN1* siRNAs in the wild-type *Ler* or *clk-st* strains and in the *cmt3* or *kyp* mutant strains (Fig. 3A). However, these siRNAs were reduced to below the level of detection in *ago4-1*. We did not detect siRNAs specific for the *SUP* or *AtMu1* sequences. This may be due to the limited sensitivity of Northern blot analysis, because siRNAs to *AtSN1* (present in approximately 70 copies per genome) are probably easier to detect than siRNAs to low-copy-number genes such as *SUP* and *AtMu1* (17).

It has been shown that long siRNAs of tobacco TS SINE retroelements did not mediate resistance to a virus carrying TS SINE sequences, suggesting that, unlike the 21- to 22-nt siRNAs, long siRNAs do not participate in PTGS (17). In addition, mutants that affect RNA silencing were used to show a correlation of long siRNAs with DNA methylation. In particular, mutants in *SDE1/SGS2* (an RNA-dependent RNA polymerase), *SDE3* (an RNA helicase), and *SGS3* (a novel gene) did not suppress the accumulation of long siRNAs or affect DNA methylation of *AtSN1*, but the *sde4* mutant (not yet cloned) suppressed both long siRNAs and DNA methylation (17). *ago4* and *sde4* map to different chromosomes and are therefore not allelic (20).

Thus, *AGO4* and *SDE4* likely encode components of a silencing system that generates long siRNAs specialized for chromatin level gene silencing (Fig. 3B). Presumably, a Dicer-like enzyme (21) and possibly an RNA-dependent RNA polymerase are also involved in siRNA production. Once generated, the long siRNAs guide *KYP*-dependent histone methylation and *CMT3*- and *DRM*-dependent DNA methylation to specific regions of chromatin. The targeting of this system to transposable elements likely contributes to suppression of transposon proliferation and to genome stability.

Note added in proof: The long and short classes of small RNAs have been shown to be bona fide siRNAs and are likely made by distinct Dicer-like enzymes (22).

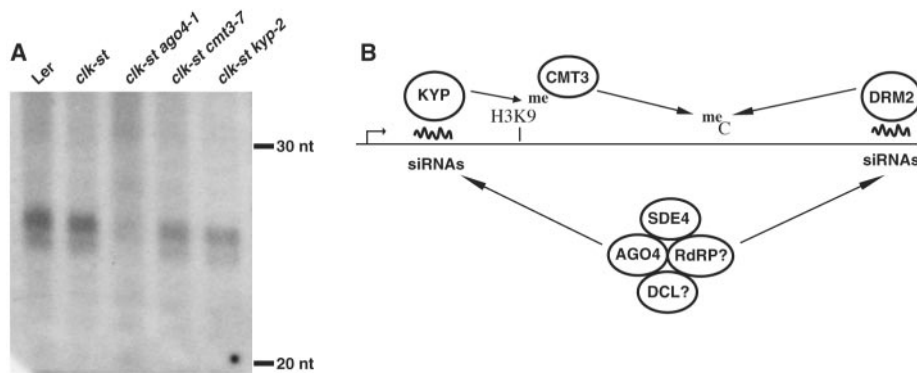


Fig. 3. Effect of *ago4-1* on *AtSN1* siRNAs. (A) Northern blot of small RNAs hybridized with a sense *AtSN1* RNA probe. ~25-nt siRNAs are found in all genetic backgrounds shown except for the *ago4-1* mutant strain. Positions of 20- and 30-nt RNA markers are indicated. (B) Model for the function of *AGO4* and long siRNAs in the control of histone and DNA methylation.

References and Notes

1. M. Fagard, S. Boutet, J. B. Morel, C. Bellini, H. Vaucheret, *Proc. Natl. Acad. Sci. U.S.A.* **97**, 11650 (2000).

2. M. A. Carmell, Z. Xuan, M. Q. Zhang, G. J. Hannon, *Genes Dev.* **16**, 2733 (2002).
3. M. Matzke, A. J. M. Matzke, J. M. Kooter, *Science* **293**, 1080 (2001).
4. J. B. Morel, P. Mourrain, C. Beclin, H. Vaucheret, *Curr. Biol.* **10**, 1591 (2000).
5. I. M. Hall *et al.*, *Science* **297**, 2232 (2002).
6. T. A. Volpe *et al.*, *Science* **297**, 1833 (2002).
7. S. Taverna, R. Coyne, C. Allis, *Cell* **110**, 701 (2002).
8. K. Mochizuki, N. Fine, T. Fujisawa, M. Gorovsky, *Cell* **110**, 689 (2002).
9. M. Pal-Bhadra, U. Bhadra, J. A. Birchler, *Mol. Cell* **9**, 315 (2002).
10. S. E. Jacobsen, E. M. Meyerowitz, *Science* **277**, 1100 (1997).
11. X. Cao, S. E. Jacobsen, *Curr. Biol.* **12**, 1138 (2002).
12. A. M. Lindroth *et al.*, *Science* **292**, 2077 (2001).
13. J. P. Jackson, A. M. Lindroth, X. Cao, S. E. Jacobsen, *Nature* **416**, 556 (2002).
14. L. Cerutti, N. Mian, A. Bateman, *Trends Biochem. Sci.* **25**, 481 (2000).
15. W. J. Soppe *et al.*, *Mol. Cell* **6**, 791 (2000).
16. X. Cao, S. E. Jacobsen, *Proc. Natl. Acad. Sci. U.S.A.*, DOI/10.1073/pnas.162371599 (2002).
17. A. Hamilton, O. Voinnet, L. Chappell, D. Baulcombe, *EMBO J.* **21**, 4671 (2002).
18. T. Singer, C. Yordan, R. A. Martienssen, *Genes Dev.* **15**, 591 (2001).
19. L. M. Johnson, X. Cao, S. E. Jacobsen, *Curr. Biol.* **12**, 1360 (2002).
20. D. Baulcombe, personal communication.
21. S. E. Schauer, S. E. Jacobsen, D. W. Meinke, A. Ray, *Trends Plant Sci.* **7**, 487 (2002).
22. G. Tang, B. J. Reinhart, D. P. Bartel, P. D. Zamore, *Genes Dev.* **17**, 49 (2003).

23. Supported by NIH grant no. GM60398 and Beckman Young Investigator and Searle Scholar awards to S.E.J. and by an NIH training grant (no. GM07185) to D.Z. We thank L. Johnson for advice on ChIP assays; C. David Allis for antibodies; A. Hamilton and M. Matzke for advice on siRNA analysis; and K. Kim, J. Chung, H. Norem, C. Hyun, and L. Do for technical assistance.

Supporting Online Material

www.sciencemag.org/cgi/content/full/1079695/DC1
Materials and Methods

Fig. S1

Table S1

References and Notes

23 October 2002; accepted 17 December 2002

Published online 9 January 2003;

10.1126/science.1079695

Include this information when citing this paper.

Modulation of Heterochromatin Protein 1 Dynamics in Primary Mammalian Cells

Richard Festenstein,^{1*} Stamatis N. Pagakis,² Kyoko Hiragami,¹ Debbie Lyon,³ Alain Verreault,³ Belaid Sekkali,⁴ Dimitris Kioussis⁴

Heterochromatin protein 1 (HP1 β), a key component of condensed DNA, is strongly implicated in gene silencing and centromeric cohesion. Heterochromatin has been considered a static structure, stabilizing crucial aspects of nuclear organization and prohibiting access to transcription factors. We demonstrate here, by fluorescence recovery after photobleaching, that a green fluorescent protein–HP1 β fusion protein is highly mobile within both the euchromatin and heterochromatin of ex vivo resting murine T cells. Moreover, T cell activation greatly increased this mobility, indicating that such a process may facilitate (hetero)chromatin remodeling and permit access of epigenetic modifiers and transcription factors to the many genes that are consequently derepressed.

The role of HP1 (1, 2) in heterochromatin formation and function was revealed by studies of position effect variegation (PEV) in which a gene juxtaposed to a heterochromatic region is stochastically silenced in a proportion of the cells that normally would express it (3–5). The probability of silencing in PEV is regulated by the concentration of heterochromatin components such as HP1 β (6, 7) or SU(VAR)3-9, a methyltransferase enzyme (8, 9) that methylates the Lys⁹ on the histone H3 tail (10, 11), creating an HP1 β binding site (12, 13). Silencing in PEV correlates with

decreased accessibility of the affected gene to nucleases (5, 7, 14). Because HP1 β is an integral component of H3 Lys⁹-methylated chromatin and therefore is thought to restrict access to factors required for crucial processes (for example, transcription, replication, repair), it is essential to know (i) whether the binding of HP1 β to chromatin is static or dynamic and (ii) whether this binding can be modulated physiologically. To address these questions, we established an in vivo mamma-

lian system to measure HP1 β mobility within heterochromatin and euchromatin in resting and activated primary murine T cells.

To use fluorescence recovery after photobleaching (FRAP) as a measure of the mobility of HP1 β in living cells, we generated transgenic mice that express a green fluorescent protein (GFP)–HP1 β chimeric protein in T cells by using a fusion cDNA construct (15) under the control of the human CD2 locus control region (16, 17). We established lines expressing GFP-HP1 β at <10% the level of endogenous HP1 β protein (fig. S1). Flow cytometry confirmed T cell–specific transgene expression and normal T cell development (that is, normal proportions of T cells in the subpopulations identified by CD4 and CD8 staining). Microscopy (18) of ex vivo T cells showed GFP signal concentrated in several discrete regions in the nucleus that colocalized with 4',6-diamidino-2-phenylindole (DAPI)–dense staining (Fig. 1). Such DAPI-dense regions have been found to colocalize with heterochromatic centromeric clusters that bind endogenous HP1 β in murine lymphocytes (19). HP1 α staining of transgenic T cells revealed similar colocalization of DAPI- and GFP-dense regions (fig. S2). A smaller amount of green fluorescence was seen throughout the rest of the T cell nuclei. These euchromatic regions, which stained densely with antibody against acetylated histone H3 (fig. S3), are likely to contain both chromatin-bound and free HP1 β .

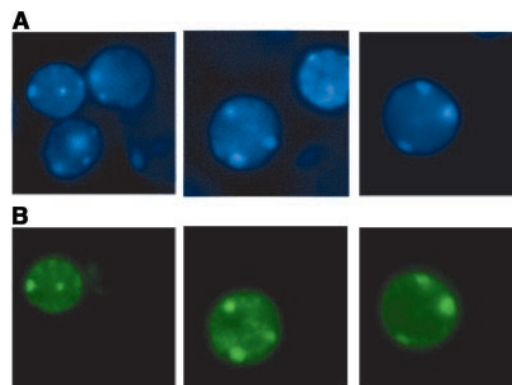


Fig. 1. GFP-HP1 β protein is concentrated in heterochromatic foci in transgenic T cells, as shown by (A) DAPI staining (blue) and (B) GFP fluorescence (green). This confirms that the GFP-HP1 β protein is localized to heterochromatic foci, as is the case for endogenous HP1 β . In addition, the regions between these foci contain lower levels of green fluorescence, indicating that GFP-HP1 β is also present in “euchromatic” areas. Non-T cells have very little green fluorescence, indicating that the background levels are low.

¹CSC Gene Control Mechanisms and Disease Group, Division of Medicine, Imperial College School of Medicine, Hammersmith Campus, Du Cane Road, London W12 0NN, UK. ²Confocal and Image Analysis Laboratory, National Institute for Medical Research, The Ridgeway, Mill Hill, London NW7 1AA, UK. ³Chromosome Dynamics Laboratory, Cancer Research UK, London Research Institute, Clare Hall Laboratories, Blanche Lane, South Mimms, Potters Bar, Hertfordshire EN6 3LD, UK. ⁴Division of Molecular Immunology, National Institute for Medical Research, The Ridgeway, Mill Hill, London NW7 1AA, UK.

*To whom correspondence should be addressed. E-mail: r.festenstein@ic.ac.uk